Developmental Biology 438 (2018) 111–123

Contents lists available at ScienceDirect

Developmental Biology

journal homepage: www.elsevier.com/locate/developmentalbiology

Original research article

Revisiting the developmental and cellular role of the pigmentation gene *yellow* in *Drosophila* using a tagged allele

Hélène Hinaux[a], Katharina Bachem[a], Margherita Battistara[a], Matteo Rossi[a], Yaqun Xin[a], Rita Jaenichen[a], Yann Le Poul[a], Laurent Arnoult[b], Johanna M. Kobler[c,d], Ilona C. Grunwald Kadow[c], Lisa Rodermund[a], Benjamin Prud'homme[b], Nicolas Gompel[a,*]

[a] Ludwig-Maximilians Universität München, Fakultät für Biologie, Biozentrum, Grosshaderner Strasse 2, 82152 Planegg-Martinsried, Germany
[b] Aix-Marseille Université, CNRS, IBDM, Institut de Biologie du Développement de Marseille, Campus de Luminy Case 907, 13288 Marseille Cedex 9, France
[c] Technical University of Munich, School of Life Sciences, ZIEL – Institute for Food And Health, Liesel-Beckmann-Str. 4, 85354 Freising, Germany
[d] Chemosensory Coding, Max-Planck Institute of Neurobiology, Am Klopferspitz 18, 82152 Planegg-Martinsried, Germany

ARTICLE INFO

Keywords:
Pigmentation
Insect
Melanin
Cell trafficking
Live imaging
Pattern boundary

ABSTRACT

Pigmentation is a diverse and ecologically relevant trait in insects. Pigment formation has been studied extensively at the genetic and biochemical levels. The temporality of pigment formation during animal development, however, is more elusive. Here, we examine this temporality, focusing on *yellow*, a gene involved in the formation of black melanin. We generated a protein-tagged *yellow* allele in the fruit fly *Drosophila melanogaster*, which allowed us to precisely describe Yellow expression pattern at the tissue and cellular levels throughout development. We found Yellow expressed in the pupal epidermis in patterns prefiguring black pigmentation. We also found Yellow expressed in a few central neurons from the second larval instar to adult stages, including a subset of neurons adjacent to the clock neurons marked by the gene *Pdf*. We then specifically examined the dynamics of Yellow expression domain and subcellular localization in relationship to pigment formation. In particular, we showed how a late step of re-internalization is regulated by the large low-density lipoprotein receptor-related protein Megalin. Finally we suggest a new function for Yellow in the establishment of sharp pigmentation pattern boundaries, whereby this protein may assume a structural role, anchoring pigment deposits or pigmentation enzymes in the cuticle.

1. Introduction

Closely related animal species with a shared body plan often look strikingly dissimilar because of diverging coloration patterns. In insects, the diversification of pigmentation patterns among closely related species reaches heights, for instance in butterflies or beetles, which exploit the riches of their colorful motifs under various selection regimes (sexual selection, crypsis, predator intimidation) (Edwards et al., 2007; Kronforst and Papa, 2015; Wilson et al., 2015).

Probably because of this prevalent role of pigmentation in species morphological diversification, researchers have sought to understand how pigmentation patterns are physically built during animal development. In insects, the research on pigmentation has taken different routes over the last century. On one hand, geneticists have isolated plethora of mutants with pigmentation defects in *Drosophila* (*yellow* (Brehme, 1941; Morgan and Bridges, 1916); *ebony* (Bridges and Morgan, 1923); *black* (Bridges and Morgan, 1919; Lindsley and Grell, 1968) *ple* (Budnik and White, 1987; Jurgens et al., 1984) or *tan* (Brehme, 1941). These are particularly well represented in genetic screens, as they are easily seen and often viable under laboratory conditions. On the other hand, biochemists have deciphered the enzymatic pathways leading to pigment deposits and their intermediate metabolites. Pigments are precipitates embedded in the insect cuticle, an extra-cellular matrix composed of lipids, proteins, chitin and catecholamines, and their formation results from a complex biochemical conversion (Locke, 2001; Massey and Wittkopp, 2016; Moussian, 2010; Sugumaran and Barek, 2016; Wright, 1987). Attempts to superimpose these two layers, a biochemical pathway and a genetic network, have reached mixed results, and the function of several genes with specific pigmentation phenotypes remains unknown.

While a more complete picture of the correspondence between genes and intermediate metabolites would help understand better how pigments are made, at least two other dimensions await documentation. First, the production of pigments is a cellular process and it is

* Corresponding author.
E-mail address: gompel@bio.lmu.de (N. Gompel).

https://doi.org/10.1016/j.ydbio.2018.04.003
Received 7 February 2018; Received in revised form 28 March 2018; Accepted 6 April 2018
Available online 07 April 2018

necessary to understand where the genetic and the biochemical networks are active in a cell. Precursors circulate in the insect hemolymph, are internalized into cells, partially processed in their cytoplasm, and secreted into the forming cuticle where they are converted into pigment deposit (True et al., 1999). Where, in this general framework, are the different gene products at work? Second, the production of pigments is a developmental process, and the temporal dynamic of this process has been largely overlooked at the expense of the spatial determinants of pigment distribution (Gompel and Carroll, 2003; Wittkopp et al., 2002a). This has started to change with the developmental survey of gene expression (Sobala and Adler, 2016). RNA-seq from *D. melanogaster* pupal wings highlights temporal differences in pigmentation gene expression, shedding a new light on the dynamic of the biochemical pathways: *ebony* and *black* are expressed at high levels at the end of pupal life (96 h after puparium formation, h APF) while *yellow* mRNA levels peak at around 52 h APF (Sobala and Adler, 2016). Pigmentation itself appears in the wing blade only around 80 h APF, in the deep layers of the procuticle (Sobala and Adler, 2016) and its formation is thus intricately linked to cuticle deposition.

In an attempt to integrate different dimensions of pigment formation, we are here revisiting the developmental role of the gene *yellow*, a gene necessary – but not sufficient – for the production of black pigments in *Drosophila*. The molecular function of Yellow is unknown (Drapeau et al., 2003; Li and Christensen, 2011). It is a secreted protein (Kornezos and Chia, 1992; Wittkopp et al., 2002a). In pupal wings, it is apparently deposited in the distal procuticle, and internalized when the proximal procuticle is secreted (Riedel et al., 2011). Its expression correlates with black melanin patterns (Drapeau et al., 2003; Riedel et al., 2011; Walter et al., 1991; Wittkopp et al., 2002a), and its function is necessary for the production of black melanin (Lindsley and Grell, 1968; Nash, 1976) although it does not appear to function as an enzyme (Wright, 1987).

To survey the dynamic of Yellow protein in time and at the subcellular level in living animals, we have created a fluorescently tagged allele to produce a Yellow::mCherry fusion protein. We have used this functional allele to follow the subcellular localization of Yellow in genetic experiments aimed at interfering with trafficking at the cellular membrane. Our results indicate that Yellow is expressed in a very precise spatio-temporal pattern during *Drosophila* pupal life, shortly preceding the onset of black pigment accumulation. The protein is targeted to the extracellular compartment from the onset of its production and during most of the pupal life. However, during the last few hours of pupal life, some amount of the Yellow protein is internalized and accumulates in the cytoplasm.

2. Results

2.1. Revisiting Yellow expression pattern using a D. melanogaster $y^{mCherry}$ line

To track Yellow expression and localization in all tissues of living flies, we first generated a *D. melanogaster yellow* allele tagged with the mCherry fluorescent protein gene (Shaner et al., 2004), using the CRISPR-Cas9 technology. In brief, we created the *yellow::mCherry* fusion allele (later referred to as $y^{mCherry}$) by repairing a CRISPR-mediated double-stranded break in *yellow* exon 2 with a template containing the custom in-frame fusion (Fig. 1A, Fig. S1A, Text S1, Text S2, details in Material and Methods). Flies with a modified *yellow* locus were initially screened by PCR (Fig. S1D). Using Sanger sequencing of a portion of the modified *yellow* locus, encompassing the fragment inserted by CRISPR-mediated homologous recombination, we determined that the allele was in line with our design. We later confirmed *mCherry* integration at the *yellow* locus by genomic DNA sequencing of the *yellow::mCherry* line at a 11 × coverage (Fig. S1F–G). The sequence coverage was however insufficient and the size of the library too small to univocally prove that the insertion was unique.

To evaluate the fidelity of the $y^{mCherry}$ reporter line, we first compared its expression in pupal wings throughout development by Western blot to that of Yellow in wild-type flies. In Canton-S, Yellow was detected in pupal wings from 54 h APF onwards as a 60 kDa band using a polyclonal antibody. A faint band could sometimes be seen at 46 h APF, suggesting that the onset of Yellow expression might be around 46 h APF. Likewise, we revealed a 100 kDa band in $y^{mCherry}$ wing extracts using the same anti-Yellow antibody. Its expression follows a similar temporal dynamic as wild-type Yellow (Fig. 1B). In both wild-type and $y^{mCherry}$ extracts, the highest protein levels were reached at 62 or 70 h APF, while Yellow was barely detectable at 90 h APF. These results were consistent with our expectations of size, and with published work (Walter et al., 1991; Wittkopp et al., 2002a). We also confirmed this expression dynamic in $y^{mCherry}$ pupal wings using an mCherry antibody (not shown). We concluded that our $y^{mCherry}$ allele reports Yellow expression dynamic accurately.

We then used the $y^{mCherry}$ allele to survey Yellow expression in wholemount flies. The fluorescence pattern proved to be consistent with Yellow expression described in fixed tissue (Drapeau et al., 2003; Riedel et al., 2011; Walter et al., 1991; Wittkopp et al., 2002a). It was also consistent with reporter construct expression under the control of *yellow* regulatory regions (Gompel et al., 2005; Jeong et al., 2006; Wittkopp et al., 2002b). In pupae (Fig. 1C–F), we detected fluorescence in transversal stripes prefiguring the abdominal banding pigmentation pattern, on the dorsal thorax in 3 longitudinal stripes (trident) and at the basis of each bristle, including in the male sex combs (inset in Fig. 1E), as well as in the mouthparts. While the fluorescence is eluded by the accumulation of pigments (see below), we noticed that it persists, at least in the wings, until adulthood (Fig. 1G,H), in line with timing of pigment precursor conversion.

In addition to the epidermal expression, we surveyed Yellow::mCherry expression in the brain at different stages, as a few reports invoke its function in neurons (Bastock, 1956; Drapeau et al., 2003; Radovic et al., 2002). We identified a small number of cells that express Yellow::mCherry in the larval brain and ventral nerve chord, at least from the second larval instar (Fig. 2A–E). A similar expression in L3 brains was already reported (Drapeau et al., 2006). We also found a similar scattered pattern in the adult brain, where the expression appears to be confined to a few cells adjacent to the optic lobe lamina, and another few ventral to the suboesophagal ganglion. We did not find positive cells in the ventral nerve chord. The expression in the adult brain was reminiscent of Pigment-dispersing factor (Pdf) expression in clock neurons (Helfrich-Forster and Homberg, 1993). We re-evaluated this expression in flies combining $y^{mCherry}$, *Pdf-Gal4* and *UAS-GFP* (Park et al., 2000), and found that the clock neurons are directly neighboring the Yellow::mCherry expressing cells (Fig. 2F, G). At all stages, in the central nervous system, Yellow::mCherry expression was strong in the soma, but was also occasionally visible in cellular extensions resembling neurites. This discrete spatio-temporal pattern of Yellow expression in the brain contrasts sharply with earlier reports of a widespread expression of cytoplasmic Yellow across the 3rd instar larval brain, with upregulation in cells expressing the male forms of Fruitless proteins (Fru^{M})- (Drapeau et al., 2003; Radovic et al., 2002).

2.2. $y^{mCherry}$ functions normally to produce wild-type pigmentation

A fusion protein may alter the normal function of a gene, for instance by destabilizing the tertiary protein structure. To evaluate the consequences of the tagged allele on *yellow*'s function, we have quantified its effect on pigmentation. $y^{mCherry}$ adult flies are superficially undistinguished from the wild-type parental line used to generate this allele (Fig. 1I). Yet, pigmentation is a quantitative trait, and subtle differences in pigmentation levels may pass unnoticed. To evaluate the functionality of our $y^{mCherry}$ allele for black pigmentation, we compared wings of age-matched adult flies with different genotypes (Fig. 1J), and measured the

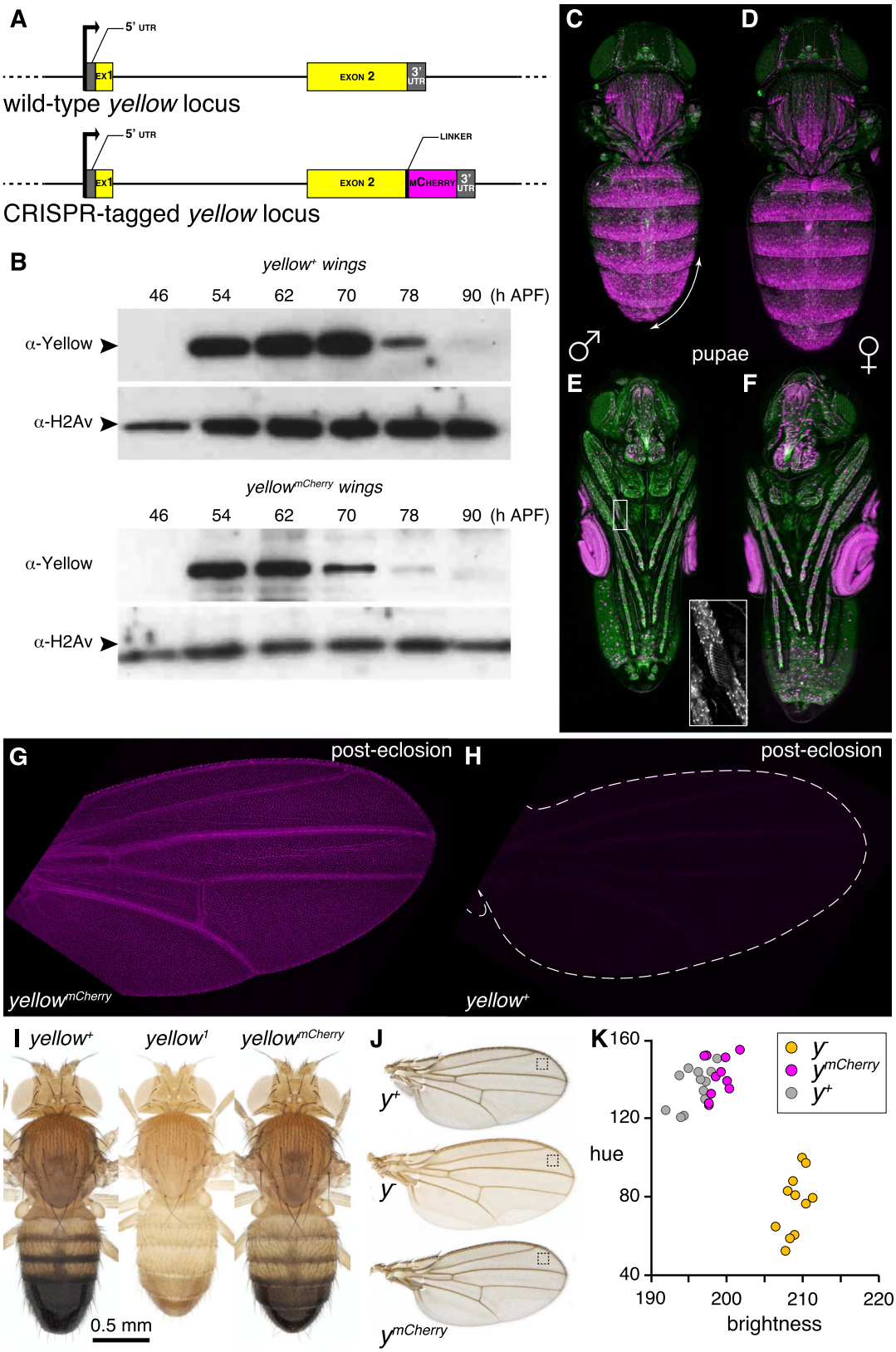

Fig. 1. A fluorescently tagged *yellow* allele. (A) Map of the *yellow::mCherry* locus compared to the wild-type *yellow* locus. *mCherry* was inserted by CRISPR/Cas9-mediated homologous recombination in frame between *yellow* exon 2 CDS and 3' UTR. A short linker sequence (Waldo et al., 1999) was added in hope to preserve the Yellow function. (B) Western blots of pupal wing protein extracts, probed with a Yellow antibody. Top: extracts from Canton-S (y^{+}) flies; bottom: extracts from $y^{mCherry}$ flies. Loading control: H2Av antibody (full gels on Fig. S1E). Of note, we detected higher molecular weight products with the Yellow antibody in pupal wings older than 62 h APF, both in Canton-S and in $y^{mCherry}$ flies (Fig. S1E). These may represent crosslinked Yellow to proteins of the maturing cuticle. (C,D,E,F) Confocal images of whole 72–74 h APF $y^{mCherry}$, utrophin-GFP male (C,E) and female (D,F) pupae, mounted dorsally (C,D) or ventrally (E,F). Anterior is up. The arrow highlights the male specific expression of Yellow throughout abdominal epidermis in segments A5-A6 (C). Note the expression in male sex combs (boxed region in (E) and higher magnification in inset). (G,H) Post-eclosion wings of $y^{mCherry}$ (I) or y^{+} (J) females, imaged under identical

confocal settings (4 wings were examined for each genotype and had identical signal to those shown). (I) $y^{mCherry}$ flies are normally pigmented. Dorsal views of 5 day-old males of the genotypes y^{+} (left), y^{1} (middle) and $y^{mCherry}$ (right) showing no difference in pigmentation color or intensity between *yellow*$^{+}$ and $y^{mCherry}$. (J) Representative wings of 5-day old males and (K) quantification of pigmentation in similar samples of the genotypes y^{+} (gray circles, n = 12), y^{1} (yellow circles, n = 11) and $y^{mCherry}$ (red circles, n = 11). Pigmentation differences were analyzed by plotting brightness against hue measured in the distal part of each wing, between the veins L2 and L3 (squares on the left panel indicate the region that was analyzed) (see methods).

levels of pigmentation (1 J,K). To this end, we have used wing color images acquired under identical conditions, encoded in an HSB color space (Joblove and Greenberg, 1978), and have plotted the hue against the brightness for each wing. This analysis confirmed that pigmentation levels and tone are identical in the wild type and in $y^{mCherry}$ flies, but strikingly different from that of *yellow* null mutants (Fig. 1K). Similarly, our quantitative analysis of abdominal pigmentation between wild type and $y^{mCherry}$ flies (not shown) revealed no difference. These results demonstrate that the Yellow::mCherry fusion protein is functional to produce normal pigmentation.

In conclusion, we have generated a functional allele of *yellow* that reports with accuracy the localization in time and space of the endogenous gene product in live animals.

2.3. Live dynamics of Yellow expression in the developing pupal wings

Although its biochemical function remains elusive, Yellow was shown to be secreted by epidermal cells (Kornezos and Chia, 1992; Riedel et al., 2011; Walter et al., 1991; Wittkopp et al., 2002a) and embedded in the cuticle. Adult cuticle is a complex layered structure, produced through the tightly regulated expression of many genes through development (Sobala and Adler, 2016). As *yellow* confers the specific dark color to the cuticle, we wondered how its developmental expression is coordinated with cuticle deposition during development. We first examined the distribution of Yellow::mCherry during development at the tissue level (this section), and then at the

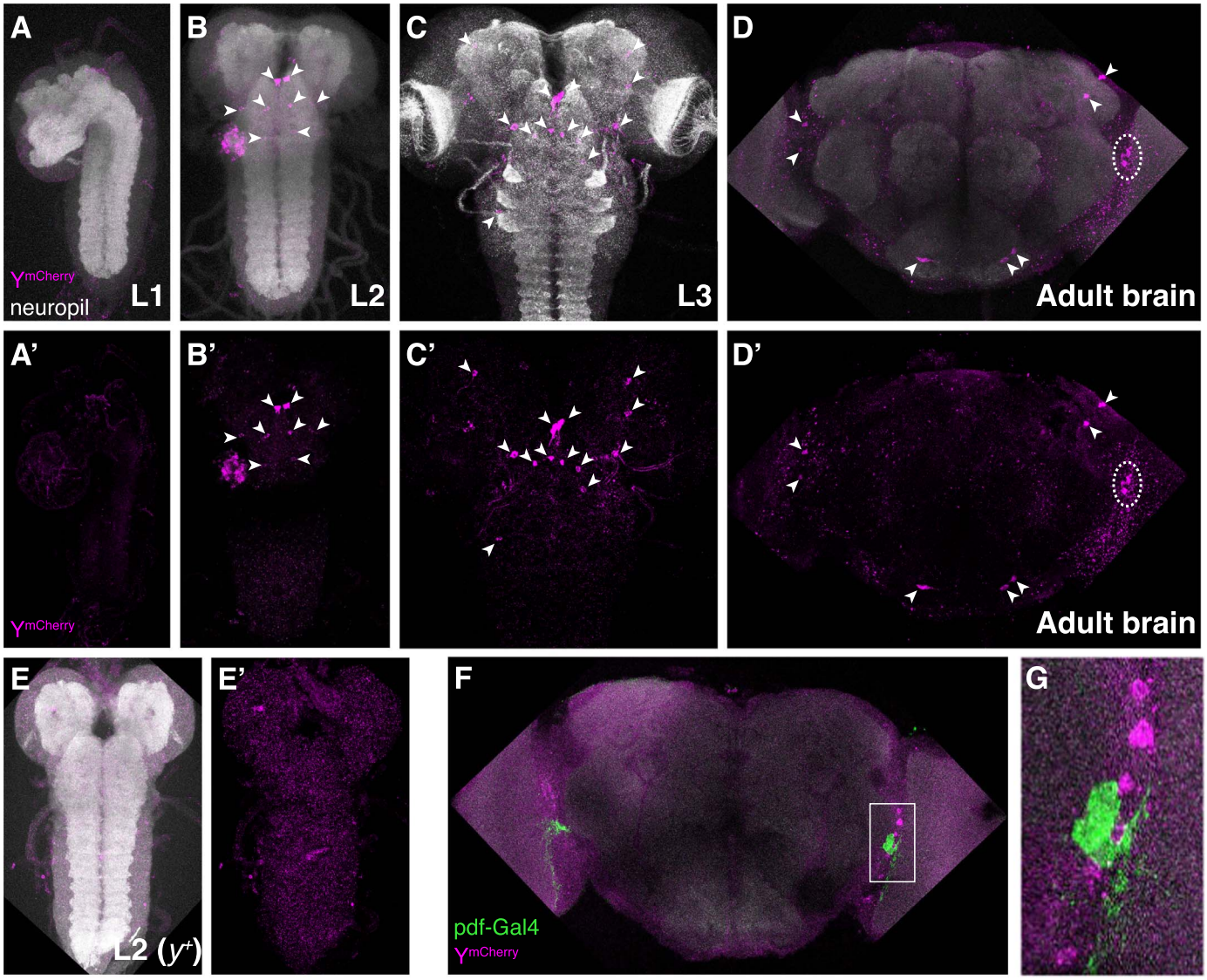

Fig. 2. Yellow is expressed in the central nervous system of *Drosophila*. Confocal projection images of larval L1 (A, A'), L2 (B, B',E, E'), L3 (C, C') and adult (D, D', F, G) brain stacks. (A–D, A'–D') Brains of $y^{mCherry}$ flies stained with an anti-N-Cadherin antibody (labeling the neuropil; shown in white) and anti-DsRed (labeling Yellow::mCherry; shown in magenta) antibody. The top line shows the merged images, the bottom line the DsRed channel alone. Arrowheads and dotted lines point to areas of Yellow::mCherry expression. (E, E') Brain of a wild-type L2 larva stained as in (B, B') confirming the specificity of the stainings in (A–D, A'–D'). (F, G) a partial brain stack projection showing clusters of Yellow::mCherry cells in the vicinity of Pdf-expressing cells (marked by Pdf-Gal4 > UAS-GFP). (G) is an high-resolution view of the region boxed in (F).

subcellular level (next section). For this and subsequent analyses, we concentrated on wings. In this tissue, it is relatively simple to follow the developmental process, from the establishment of a pigmentation gene's blueprint, to the differentiation of the actual pigments in the acellular adult wing.

We initially recorded male $y^{mCherry}$ pupae with live time-lapse imaging from 44 to 73 h APF (Fig. 3A). We then quantified the fluorescent signal in the wings (Fig. 3B–C). For all individuals (n = 3), fluorescence appeared around 50 h APF, increased rapidly until 56–59 h APF, and plateaued until 66–68 h APF. This is in agreement with the expression dynamics deduced from Western blots (Fig. 1B) and transcriptomic analysis indicating that the onset of *yellow* transcription in the wing is between 42 and 52 h APF (Sobala and Adler, 2016). Fluorescence then decreased abruptly until it was no longer visible under our imaging conditions, around 72–73 h APF. Our Western blots experiments, though, detected Yellow in the wings, albeit at lower levels, at 78 and 90 h APF (Fig. 1B). Additionally, we had detected fluorescence in $y^{mCherry}$ wings after eclosion using confocal imaging (Fig. 1G). Therefore, the fading of fluorescence from pupae was unexpected. We noted that in the time-lapse movies, the decrease in fluorescence occurred simultaneously in all pupal tissues (Movie S1), and correlated precisely with the accumulation of pigmentation (Fig. 3D–E). This suggested that Yellow::mCherry protein was still present at later pupal stages, but that the fluorescent signal was masked by pigmentation.

Supplementary material related to this article can be found online at http://dx.doi.org/10.1016/j.ydbio.2018.04.003.

In the abdominal epidermis, Yellow expression prefigures the adult banding pattern of pigmentation. From a broad, fuzzy domain in each segment, the expression refines over time to a sharp transversal band. This refinement is not synchronous across segments, but instead follows a temporal sequence from anterior to posterior segments completed after 75 h APF (Wittkopp et al., 2002a). We examined the spatial dynamic of expression in the pupal abdomen of $y^{mCherry}$ animals at 65, 70 and 75 h APF, focusing segments A3 and A4. The expression was already sharp at 65 h APF (Fig. S2A). The quantification of fluorescence intensity profiles along the segments, however, did not reveal any changes between the different stages for the A3 segment (Fig. S2C, E). For segment A4, we tentatively observed a very subtle refinement of the anterior boundary (Fig. S2B, D).

2.4. Developmental dynamics of Yellow subcellular localization

To understand how Yellow is produced in relationship to cuticle deposition, we compared the distribution of Yellow::mCherry to that of other markers in developing pupal wings: an mCD8::GFP fusion protein (Lee and Luo, 1999) to outline the cytoplasm, and an indicator of chitin production (Fig. 4). It is indeed possible to directly monitor cuticle localization in transgenic flies expressing the chitin reporter *ChtVis-Tomato* (Sobala et al., 2015, 2016). We could, however, not directly compare ChtVis-Tomato to Yellow::mCherry distribution in the same cells, as these fluorescent reporters have overlapping emission spectra. Instead, we compared their respective distributions to that of mCD8::GFP (*mCD8::GFP*, *ChtVis-Tomato* on one hand, and *mCD8::GFP*, $y^{mCherry}$ on the other hand) to infer where Yellow localizes during cuticle deposition (Fig. 4, Fig. S3) in wing cells. Yellow is not detected at 46 h APF (Fig. 4D), a stage at which chitin is already present in wing hairs (trichomes) (Fig. 4A). Yellow then accumulates in the wing blade trichomes shortly after the onset of its expression (54 h APF, Fig. 4E, Fig. S3H). Also at 54 h APF, we detect very faint Yellow::mCherry signal at the apical outline of the cells (Fig. S3S,T). This is the stage at which the envelope and the epicuticle have been deposited on the pupal wing (Sobala and Adler, 2016). At this stage, chitin still appears limited to the trichomes (Fig. 4B). Yellow::mCherry signal decreases in the trichomes between 70 and 78 h APF (Fig. 4E–F, Fig. S3J–K), possibly again because of the accumulating dark pigments (see Fig. 3D-E). Chitin is also visible, lining-up the cell contours, in addition to its presence in trichomes from 62 h APF onwards (Fig. 4C, Fig. S3C–F). At the same stage, Yellow::mCherry signal distinctly outlines cells at the apex (Fig. S3U, V), suggesting that Yellow is incorporated in the cuticle shortly after, or together with chitin. Nevertheless, at 78 h APF and even more so at 90 h APF (Fig. 5F,H, Fig. S3K,L), Yellow::mCherry accumulates into the cytoplasm. This cytoplasmic signal could in principle result either from newly expressed Yellow::mCherry that is not exported to the cuticle, or from cuticular Yellow::mCherry that is re-internalized (Riedel et al., 2011).

We concluded from these experiments that Yellow production is tightly correlated in space and time with the process of cuticle formation.

2.5. Regulation of Yellow subcellular localization

The tight timing of Yellow expression and cellular dynamics in the epidermis may reflect a structural role in the cuticle as much as its requirement for pigment production. We next investigated how Yellow subcellular localization influences pigmentation, by knocking down a gene that could control Yellow trafficking. This study, together with previous reports (Kornezos and Chia, 1992; Riedel et al., 2011; Walter et al., 1991) indicates that Yellow is secreted and later possibly reinternalized. To examine the control of this phenomenon, we sought to impair endocytosis, and examined the consequences on Yellow::mCherry and on pigment formation in the wing. Megalin, a large low-density lipoprotein receptor-related protein involved in endocytosis, is thought to control Yellow endocytosis at the end of pupal life (Riedel et al., 2011). Yet, Yellow endocytosis was studied in an ectopic context, in third instar wing discs, a tissue that normally does not express Yellow. We first confirmed that *megalin* (*mgl*) RNAi knockdown resulted in darker pigmentation and in a more fragile cuticle in the wing (Fig. 5A–B) (Riedel et al., 2011). We have quantified this overall phenotype by comparing *mgl* RNAi wings to control wings imaged under identical conditions (Fig. 5C). Because these *mgl* RNAi wings show other overall morphological differences (in particular they tend to be smaller than wild-type wings), we wondered whether their darker appearance was really the result of additional pigment deposits. We examine the coloration difference at a higher magnification and found that the density of trichomes is slightly increased in *mgl* RNAi wings (Fig. S4), and could contribute to the darker phenotype. We therefore measured the pigmentation between trichomes in the wing blade of the RNAi and control samples. We found that the cuticle is distinctly darker in the wing blade between trichomes (Fig. 5D–E). Moreover, we found that the pigmentation changes are mainly due to dark specks at the base of many trichomes. These specks are occasionally present, but smaller and fainter, in control wings. Interestingly, this phenotype is mirrored in the cellular accumulation of Yellow::mCherry in *mgl* RNAi wings (see below).

Crossing a *mgl* RNAi transgenic line to our $y^{mCherry}$ line allowed us to directly visualize the effect of *mgl* knockdown on Yellow localization. At 70 h APF, in control wings, Yellow is mainly located in trichomes (Fig. 5F). In *mgl* RNAi wings, Yellow signal is present in trichomes, but also in spots at the cell surface – either in the cuticle between the trichomes or close to the membrane (Fig. 5G). At 90 h APF, when Yellow signal is barely detectable in wing hairs in control wings, it is still strong in *mgl* knockdown (Fig. 5H–I). It is also still present in aggregates at the apical cell surface. These Yellow aggregates (Fig. 5G,I) are reminiscent of the dark pigmentation specks seen in adult *mgl* RNAi wings (Fig. 5D). We concluded that in the absence of Mgl, high amounts of Yellow accumulate at the apical outline of the cells, not just in trichomes, leading to the production of dark specks. In line with this increased accumulation of Yellow in the cuticle of *mgl* RNAi wings, we also noted that at 90 h APF, Yellow::mCherry signal in the cytoplasm is stronger in control wings than in *mgl* RNAi wings, although we didn't

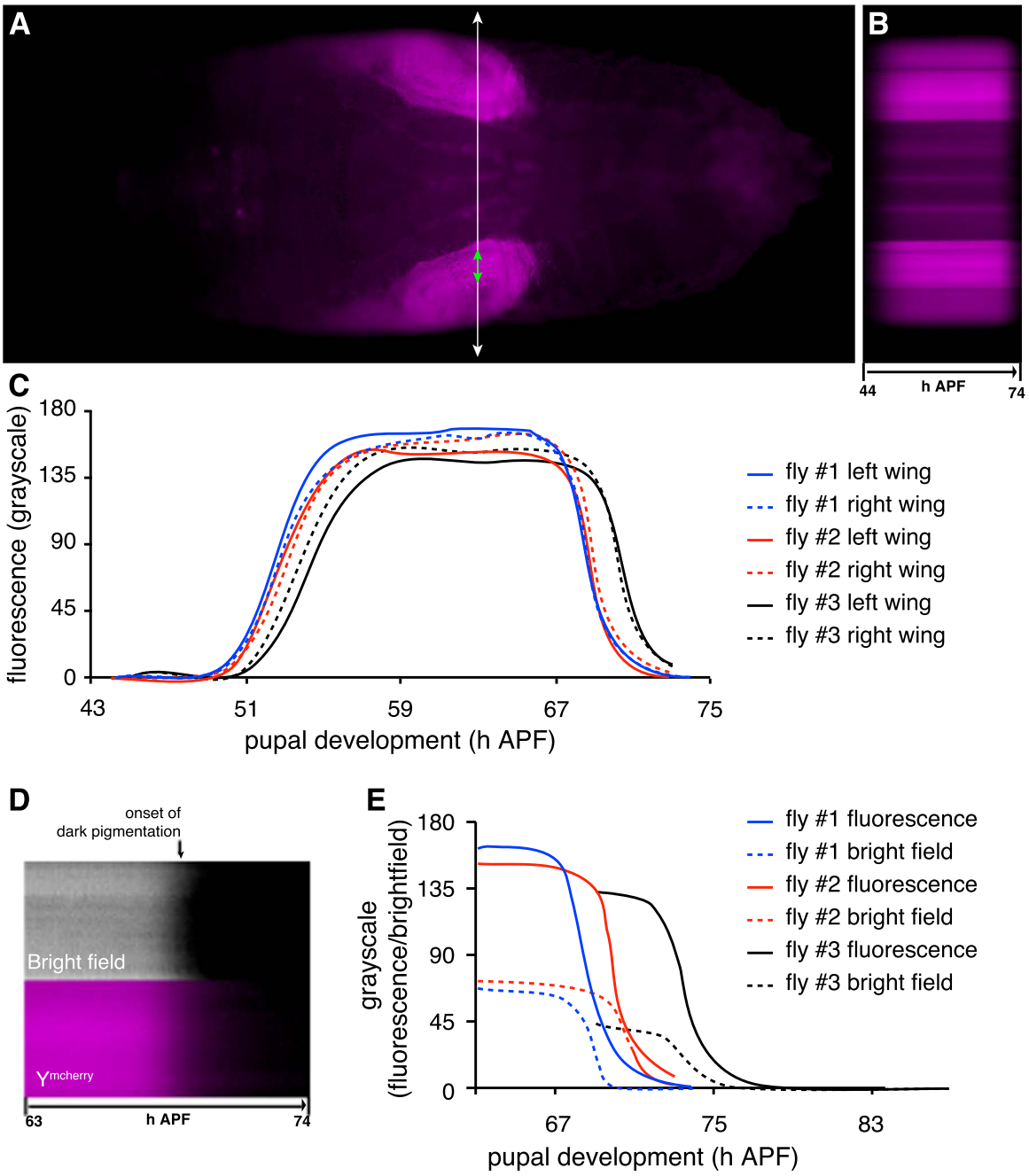

Fig. 3. Live temporal dynamics of Yellow expression in the developing pupal wings. (A) Still frame of a live male $y^{mCherry}$ pupa imaged in time-lapse from 44 to 74 h APF. (B) Chronogram showing the variation of fluorescence intensity during development for one particular position along the antero-posterior axis at the level of the wings as shown by a white line on panel (A). (C) Quantification of fluorescence intensity in the wings of 3 $y^{mCherry}$ male pupae imaged with the same time-lapse settings. (D) Chronograms of the same $y^{mCherry}$ male pupa as in A at the level of the wing (see green arrow in A) for brightfield (top) and fluorescence (bottom) between 63 and 74 h APF. Note the correlation of pigmentation appearance and fluorescence decline (arrow). (E) Quantification of fluorescence and brightfield intensities in 3 $y^{mCherry}$ male pupae, showing some variability in pigmentation appearance. Of note, brightfield settings could not be adjusted finely to be identical, which explains the differences in maximum brightfield intensity between pupae.

find this difference to be statistically significant (Fig. 5H–J). These results reinforce the notion that Mgl is involved in the internalization of Yellow from the cuticle at the end of pupal development, thereby regulating its amount and cuticular embedding for dark pigment production.

2.6. A structural role of Yellow in the cuticle?

The expression and cellular trafficking of Yellow, its regulated embedding in the cuticle produced by a given cell, result in a variety of pigmentation phenotypes at the level of an entire animal. These include light homogeneous gray dusking of certain body parts, but also specific pigmentation patterns characterized, in the fly, by a steep transition from the background to the pigmented area. In addition to imparting dark pigmentation to these patterns, Yellow has been proposed to act as a cuticular anchor for pigmentation, around which phenol oxidases, as well as other enzymes, would irreversibly cross link catecholamines to cuticular compounds (Walter et al., 1991). If this anchor model is correct, catecholamines should diffuse more in Yellow's absence, and one would expect *yellow* mutants to display fuzzier pattern boundaries. To test this hypothesis, we examined another *Drosophila* species, *D. biarmipes*, whose males harbor a solid spot of dark pigments (Fig. 6A). We have isolated a *yellow* null mutant from this species (Arnoult et al., 2013). A wing spot remains visible in

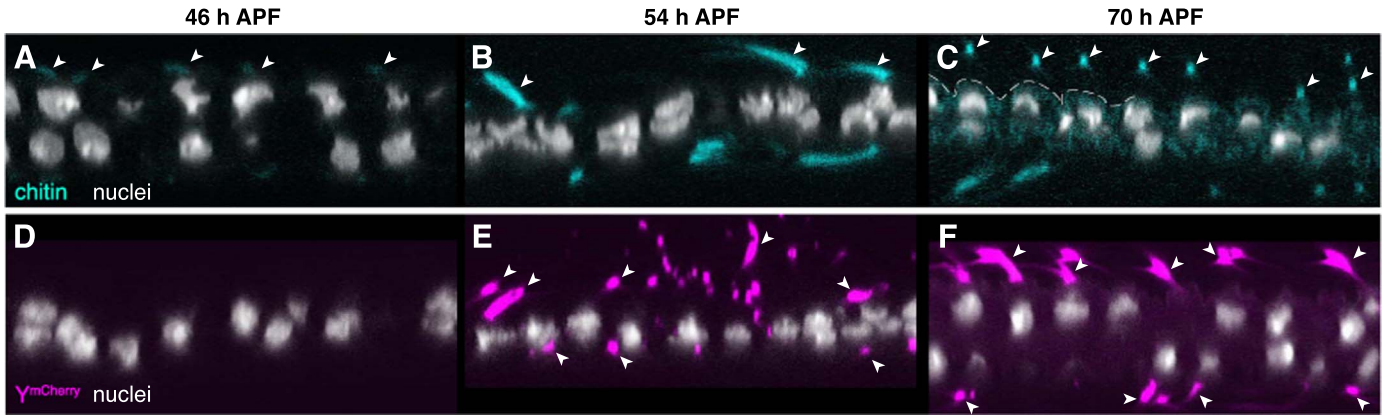

Fig. 4. Temporal dynamics of Yellow subcellular localization in the developing wing. Optical confocal sections through *ChtVis-Tomato* pupal wings (A-C) and $y^{mCherry}$ pupal wings (D-F) at 46 (A, D), 54 (B, E) and 70 h APF (C, F). ChtVis-Tomato, which labels chitin, was imaged with the same settings at all stages and is shown in blue. Yellow::mCherry was imaged with the same settings at all stages and is shown in magenta (n = 3 for each stage and genotype). Nuclei are marked with DAPI (white). Arrowheads point to expression in the trichomes. The dotted line in C highlights the enrichment of ChtVis-Tomato at the apical outline of the cells.

y^- males (Fig. 6B), yet it is faint and no longer dark. The background pigmentation is also reduced throughout the wing. The overall location of the pigmentation pattern is, however, similar. We compared the profile of average pigmentation intensity at the transition from the wing background to the spot between y^- and wild-type males (Fig. 6E, see methods). This analysis first showed that the profiles were more variable inside the spot for the y^- wings, both within and accross individuals. Because the wing background pigmentation is more than 3 times less intense in the y^- compared to wild type, we could not compare the global slope of the profile without introducing major biases. Nevertheless, at the outer edge of the more pigmented area in y^- flies, the pigmentation levels were consistently higher compared to wild

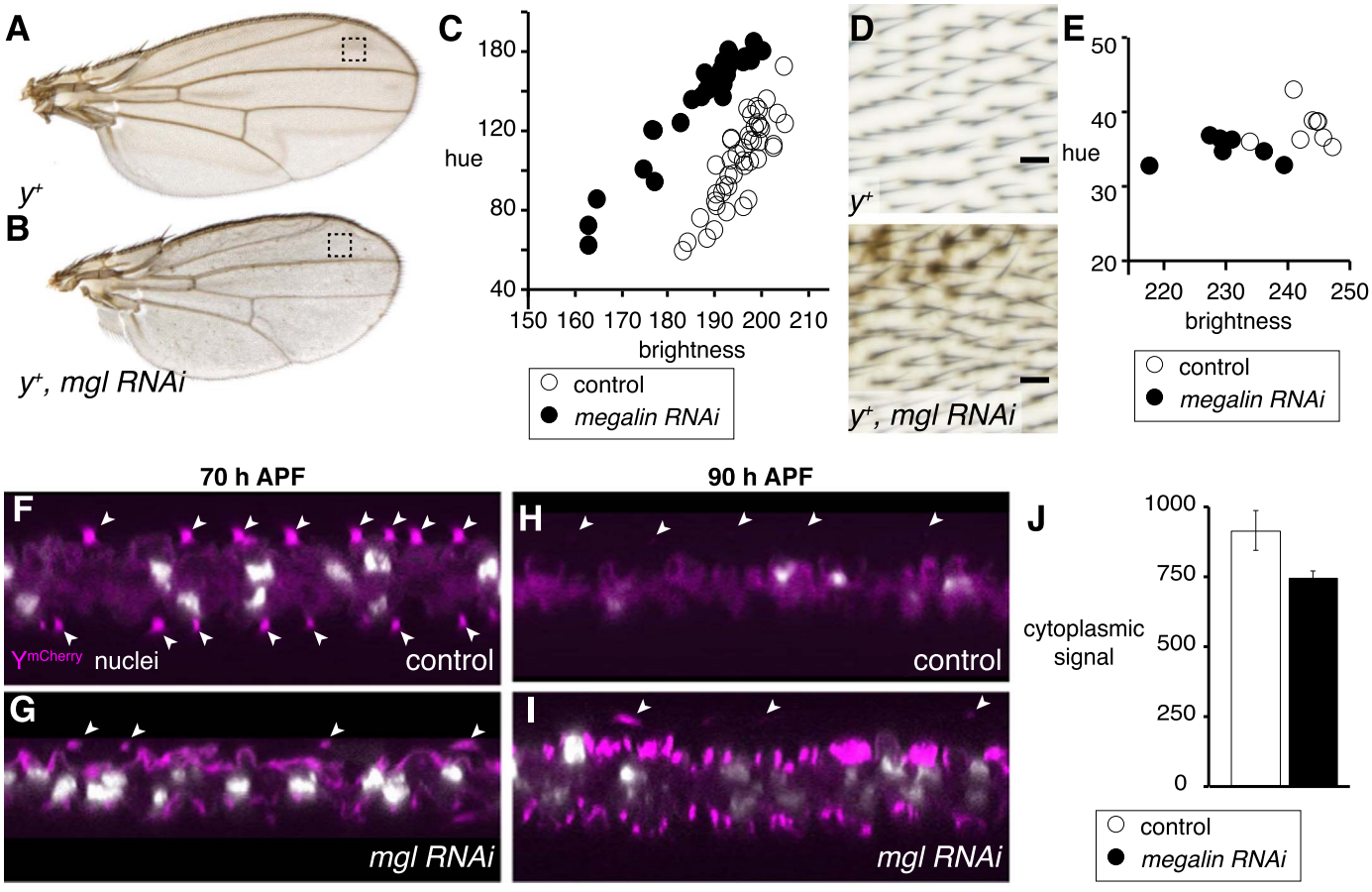

Fig. 5. Megalin controls pigmentation levels in the wing through reinternalization of Yellow. (A-B) Representative wings of 5-day old males of the genotypes y^+,*UAS-mgl-shRNA* (A) and y^+, *NP3537 > UAS- mgl-shRNA* (B). (C) Quantification of pigmentation in samples of the genotypes y^+ (control, white circles, n = 44) and y^+, *NP3537 > UAS- mgl-shRNA* (black circles, n = 31). Pigmentation differences were analyzed by plotting brightness against hue measured in the distal part of each wing, between the veins L2 and L3 (box in A, B) (see methods). (D) Details of representative y^+,*UAS-mgl-shRNA* control (top) and y^+, *NP3537 > UAS- mgl-shRNA* wings (bottom) showing pigmentation specks at the basis of some trichomes (scale bar: 10 μm). (E) Quantification of pigmentation between trichomes in such pictures (n = 8 wings of each genotype, each wing sampled with 4 20-pixel squares). (F-I) Optical confocal sections through pupal wings of the genotype $y^{mCherry}$ (F,H) and $y^{mCherry}$ *NP3537 > UAS-mgl-shRNA* (G,I) at 70 (F,G) and 90 h APF (H,I). Yellow::mCherry was imaged with the same settings at all stages and is shown in magenta (n = 5 for each stage and genotype). Nuclei are marked with DAPI (white). Arrowheads point to expression in the trichomes. (J) Quantification of cytoplasmic Yellow::mCherry signal (n = 5 wings of each genotype, each wing sliced 3 times and each slice sampled with 20 30-pixel squares).

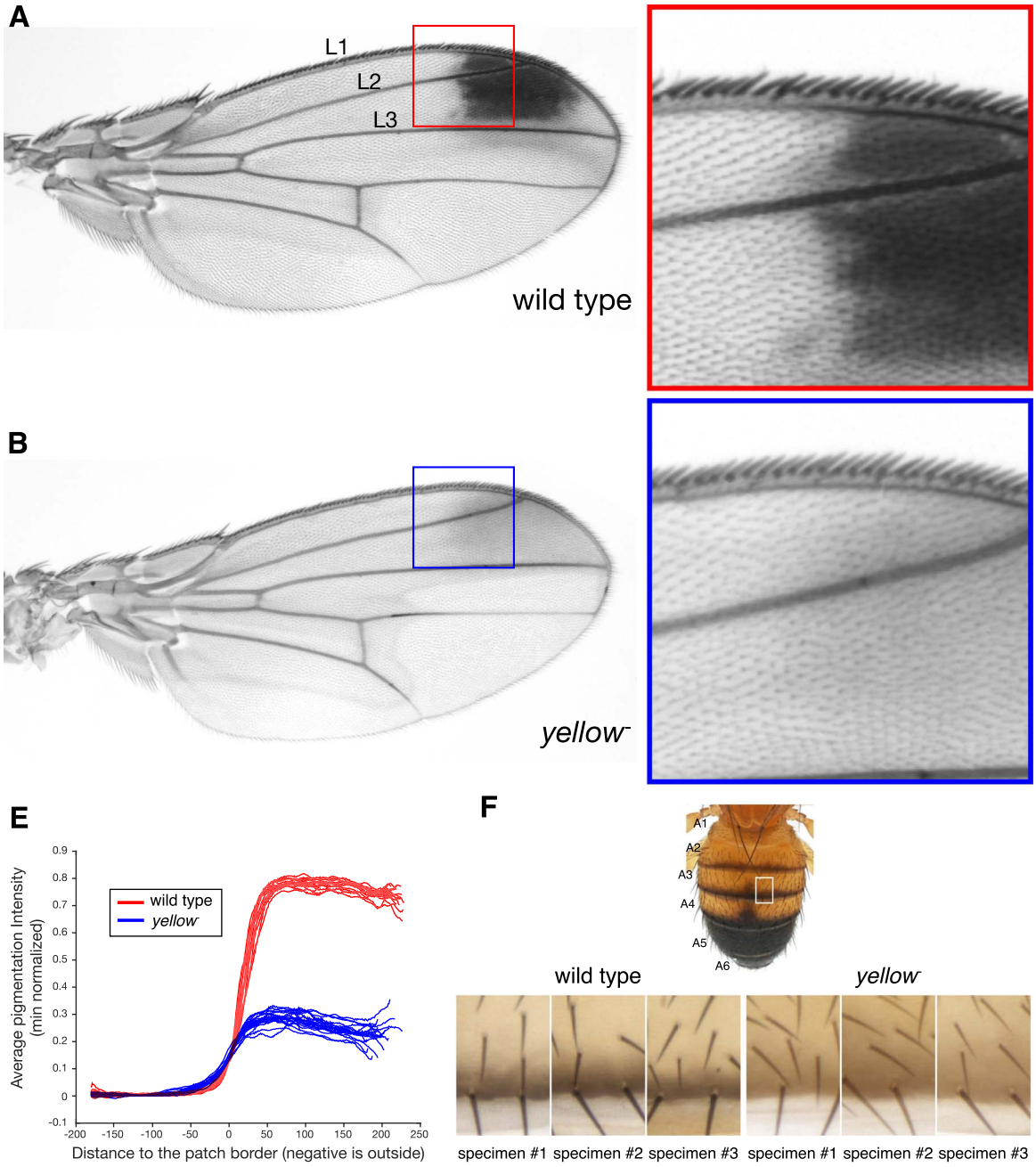

Fig. 6. Pigmentation intensity profiling at wing spot boundary between wild-type and *yellow D. biarmipes* males. (A–B) Representative wings of 5-day old *D. biarmipes* males of the genotypes y^+ (A) and y^- (B). L1-L3 indicate veins referred to in methods. (C–D) Higher resolution views of the regions boxed in (A, B). (E) Profiling of pigmentation intensity at the transition between wing background and spot area after alignment of 16 wild-type (red) and 11 y- (blue) wings, and normalization of the lower values (see methods). (F) Picture of a male *D. biarmipes* abdomen (top), showing the portion of A3 segment that was compared between y^+ and y^- samples (bottom).

type, suggesting that the pattern was more diffuse in *yellow*$^-$ (Fig. 6E, Fig. S5). We then used the same flies and examined the boundaries of the banding pigmentation pattern on their abdomen (Fig. 6F). Comparing the anterior boundary of a band on segment A3 for instance between wild-type flies and y^- mutants also shows a striking difference in the sharpness of the pattern boundary. While the boundary is sharp and parallel to the anterior border of the segment in the wild type, it is fuzzy and irregular in the mutant, resulting in a broader band.

We concluded from these results that, in addition to contributing a dark hue to pigmentation, Yellow may also play a role in anchoring pigment deposits into the cuticle. Alternatively, we cannot exclude that the pigments produced in a *yellow* mutant are more mobile by nature than the black pigment deposits characteristic of the wild type, and explain the apparent dispersion that we describe above.

3. Discussion

3.1. Understanding pigment formation in time and space, and from cell resolution to tissue level phenotype

The literature on pigment formation in insects focuses largely on the biochemistry of this process (Czapla et al., 1990; Sugumaran and Barek, 2016; Wright, 1987), as well as on the spatial control of pigment deposition at the level of tissues (Kronforst et al., 2012; Wittkopp et al., 2003). The temporal and developmental dimension of pigment formation, as well as the cellular processes leading a structure to be colored are generally not well understood. But perhaps more limiting to understand the process of pigment formation, very few studies attempt to connect these different dimensions: development, cellular processes, tissue

patterning and molecular function. In an attempt to connect these dimensions, our motivation with the present work was to focus on a key determinant of black pigment formation in *Drosophila*, *yellow*, and analyze its contribution from cell to tissue across development. The generation of a functional, fluorescent protein-fusion *yellow* allele allowed us indeed to examine the process of pigment formation over developmental time. By doing so, we collected direct information on the dynamics of Yellow expression and cellular targeting in relationship to the process of cuticle deposition. We found that in the wing Yellow is exported to the apical membrane at the level of trichomes soon after the cuticle envelope and the trichomes have formed, at the onset of epicuticle secretion (52 h APF) (Sobala and Adler, 2016). Following endogenous Yellow trafficking over development in the wing, we also confirmed that the excess of protein is reinternalized by the epidermal cells (Riedel et al., 2011). In the wing, these cells later disappear (Kiger et al., 2007), and the balance of Yellow levels is therefore set during pupal development. If this process does not take place properly, we found that Yellow accumulates in patches, presumably in the cuticle, and that this accumulation correlates with specks of pigmentation at the base of trichomes of the adult wing, explaining the overall darker color of the wings. In this way, our results do integrate the description of a cellular process over developmental time, and its overall phenotypic consequences on the animal body.

In line with previous work, our study showed how Yellow protein levels in the adult cuticle are determined by regulated developmental processes impacting the final color. The embedding of Yellow in the cuticle may also assume a structural role in the establishment of pigmentation patterns (Drapeau, 2003; Li and Christensen, 2011; Walter et al., 1991). In *Drosophila*, as in many other insects, the animal emerging from a pupa is pale, or completely unpigmented. Pigment pattern develop in the hours to days following eclosion. They result from diffusing pigment precursors being locally converted into colored precipitates (True et al., 1999). These pigment deposits are not thought to be diffusible, but it is conceivable that they nevertheless spread over a few cell diameters over time. In that respect, using mosaic gynandromorphs, Hannah (Hannah, 1953) showed that cuticle and bristles of y^- genotype could have wild-type pigmentation when located in the vicinity of wild-type, Yellow-expressing, clones. She interpreted this result as the diffusion of pigment-producing substances. It may indicate that wild-type Yellow protein diffuses in the cuticle after being produced from wild-type clones, or that black melanin diffuses in the cuticle after its conversion in the cuticle of wild-type clones. Her experiments however were not designed to answer the question of whether pigments and/or pigment-producing enzymes diffused faster in the cuticle in the absence of Yellow. Pigment patterns, in particular in insects, are characterized by sharp boundaries. The proteins involved in pigment precursor conversion may also stabilize pigment deposits, and thereby contribute to sharper pattern boundaries. We explored this possibility by examining the edge of a pigmentation pattern element in *Drosophila* wings. Our results show that the boundary becomes fuzzy in the absence of Yellow, consistent with an anchoring, structural role of this protein in pigment deposition. Yellow, through its cysteine and methionine residues, could cross-link 5,6-indole quinones in the cuticle (Geyer et al., 1986). Melanins are usually found associated with proteins (Mason, 1955), and Yellow could be associated to dopamine-melanin (Gibert et al., 2017). In its absence, either an altered form of melanin would be produced, or indole-5,6-quinones would self-polymerize in the presence of beta-alanine, resulting in the formation of a tan instead of black pigment (Sherald, 1980). However, no structural protein interacting with 5,6-indole quinones has been identified to date in any species (Sugumaran and Barek, 2016).

3.2. Yellow, a pleiotropic gene with a neuro-developmental function

The diversification of pigmentation pattern in *Drosophila* is intimately and recurrently related to changes in the transcriptional regulation of *yellow*, rather than in its coding sequence (Arnoult et al., 2013; Gompel et al., 2005; Jeong et al., 2006; Prud'homme et al., 2006; Rebeiz et al., 2009; Werner et al., 2010; Williams et al., 2008). This mode of evolution is presumably imposed by the pleiotropic effects of mutations in its coding sequence, not tolerable by natural selection. While a change in the regulation of *yellow* expression may affect this or that pattern element, it is immediately clear that a *yellow* protein mutant is globally changing color (Fig. 1I). Adding to the pleiotropy hypothesis, several studies have invoked a behavioral function for this gene, in particular during male courtship (Drapeau et al., 2006). Yet, the neuronal correlate of this behavior remains elusive. Indirect evidence show that a 300 bp regulatory element may control *yellow* expression in two neurons of the larval brain (Drapeau et al., 2006), but it remains unclear whether the lack of *yellow* expression in two neurons of the larval brain compromises male courtship circuitry, or whether *yellow* is expressed later on in the adult brain, in neurons affecting aspects of the male courtship, including wing extension (Bastock, 1956). Using our tagged allele, we explored Yellow expression in the nervous system across the fly life cycle. We confirmed the L3 larval expression in a small subset of cells, not just 2, scattered in the brain and the ventral nerve chord (Drapeau et al., 2006). We also found a similar expression pattern earlier on during larval life, and later on, in the adult. *yellow* has been implicated in the control of male courtship, but the neuronal correlate of this function remains elusive. One could expect Yellow expression in the brain to be dimorphic, or to overlap with Fru^M expression (Stockinger et al., 2005) or both. Our results do not indicate that Yellow distribution is dimorphic in the brain, and its comparison to the published expression of Fru^M does not suggest overlap. At the cellular level, it is also strikingly different from that of epidermal cells: Yellow is confined to the cell cytoplasm in the brain, suggesting a differential mode of production or cellular addressing. Our results deepen the mystery of *yellow* function in the brain, but open the door to the survey and identification of specific neuronal drivers to analyze the role of *yellow* in behavior.

4. Material and methods

4.1. Fly cultures

All stocks were grown on standard cornmeal medium. *M{Act5C-Cas9, 3XP3-RFP, w^+}ZH-2A, w^{1118}* was a gift from Frank Schnorrer's lab (Port et al., 2014). *w*; nab-Gal4^{NP3537}, tub-Gal80^{ts} / TM6, Sb, Tb* is a wing-specific driver active throughout development (Arnoult et al., 2013; Pavlopoulos and Akam, 2011). *w*, UAS-ChtVis-Tomato* line was a gift from Paul Adler's lab (Sobala et al., 2015). *w*; sqh-utrophin::GFP* (Rauzi et al., 2010) was a gift from Anne Classen. Other lines were obtained from the Bloomington Drosophila Stock Center (BDSC), the Vienna Drosophila Resource Center (VDRC), or derived from these stocks with the following references:

(1) Canton-S
(2) *w**
(3) *y^1 w*; UAS-mCD8::GFP* (Lee and Luo, 1999).
(4) *UAS- mgl-shRNA* (VDRC #27242).
(5) *P{w[+mC]=Pdf-GAL4. P2.4}X, y[1] w[*];;* (Park et al., 2000)

4.2. Molecular biology

4.2.1. Repair construct

Part of the *yellow* locus (intron, exon2, 3′ UTR and 3′ intergenic sequence) was amplified from wild-type *D. melanogaster* genomic DNA using the primers: yFE (CAA TGC TGG GCT CAA TTG GA) and yRI (GCC TGC TCT TTG TTC CTC TG). The resulting amplicon was cloned into a *pJet1.2* plasmid (ThermoFisher Scientific). The *pJet-yellow* vector was digested with *Hpa*I (NEB) and used for an InFusion reaction (CloneTech) with an amplicon consisting in the mCherry

sequence with a 5′ linker (Waldo et al., 1999). This amplicon was generated by PCR on the pTV-Cherry vector (Baena-Lopez et al., 2013) (a gift from Jean-Paul Vincent) using the primers InFusion-F2 (ATC ATC AGC ATC AAG GTT CCG CTG GCT CCG CTG CTG GTT CTG GC) and InFusion-mCherry-Rev (CCGTGTGTAGGATTATGTTACTTGTACA GCTCGTCCATGCC). The *pJet-yellow-mCherry* vector was then mutated at the target site of sgRNA F4 (see below) to minimize risks of cuts (synonymous mutations). Two amplicons were generated by PCR on the *pJet-yellow-mCherry* vector (using primers mel_y_*Pac*I_Fw (GGA ATT TAG GCA GAA ATT CCA G) / mel_y_mut_Rv (TCG AAT CCT CGT ATC CGT GGT CAA) and mel_y_mut_Fw (AGG ATT CGA AGA TAC GAG CTA CCT G) / mel_y_*Stu*I_Rv (GTG CTG GTT GAA AAT ATA GGC C)). The 2 PCR products were combined by overlap extension PCR, to generate a mutated *Pac*I-*Stu*I fragment. In parallel, the *pJet-yellow-mCherry* vector was digested by *Pac*I and *Stu*I and used for an InFusion reaction (CloneTech) with the mutated *Pac*I-*Stu*I fragment. This resulted in a *pJet-yellow_F4mut-mCherry* vector, hereafter called the repair construct (sequence in Text S1).

4.2.2. sgRNA

The sgRNA y2 (GGA TGA GTG TGG TCG GCT GTG TTT TAG AGC TAG AAA TAG CAA GTT AAA ATA AGG CTA GTC CGT TAT CAA CTT GAA AAA GTG GCA CCG AGT CGG TGC TTT T) was described by Bassett and colleagues (Bassett et al., 2013). The sgRNA F4 (GGT GAC CAC GGA TAC GCG AAT TGT TTT AGA GCT AGA AAT AGC AAG TTA AAA TAA GGC TAG TCC GTT ATC AAC TTG AAA AAG TGG CAC CGA GTC GGT GCT TTT) was designed using www.flyrnai.org/crispr2 (Housden et al., 2015). Both sgRNAs were produced as described (Bassett and Liu, 2014).

4.3. Embryo injections

505 embryos of the y^{+}, *M{Act5C-Cas9, 3XP3-RFP,* w^{+}*}ZH-2A,* w^{1118} line were injected with water solution of sgRNA y2 at 40 ng/µL. 105 G0 adults were screened, 92 showed mosaic *yellow* clones. 4 independent *yellow* mutant lines ($y^{CRISPR\ y2}$) were recovered (Fig. S1C). 1164 embryos $y^{CRISPR\ y2}$, *M{Act5C-Cas9, 3XP3-RFP,* w^{+}*}ZH-2A,* w^{1118} line were injected with a dilution of the sgRNA F4 (80 ng/µL) and the repair construct *pJet-yellow_F4mut-mCherry* (150 ng/µL). 71 G0 adults were screened, 5 showed mosaic wild-type clones. Among them, two had wild-type pigmented flies in their progeny, from which lines were established. We extracted genomic DNA from these lines and ran a diagnostic PCR (y-mel-ex1-Fw (AAG CCA CCT GAT TAC CCG AA)/y-insert-Rv2 (CAC GAT GAC TGA TGT GTG GT)) to confirm the repair (Fig. S1D). A portion of the *yellow* locus was then amplified (y-intron-Fw (AGC AAA TCG GTA GTG GCA AC)/y-insert-Rv2 (CAC GAT GAC TGA TGT GTG GT) and cloned into a pCR™8/GW/TOPO™ vector (ThermoFisher Scientific) which was sequenced with Sanger technology at Eurofins genomics. This showed that the whole repair sequence was introduced, with no mutation, at the endogenous *yellow* locus, as the fragment cloned was larger on the 5′ end than the homology arm.

4.4. Genome sequencing

The genomic DNA of 40 females from the $y^{mCherry}$ line was purified using the Blood and Cell Culture DNA Midi kit (Qiagen). The library was prepared using the 1 S Plus Kit (Swift Biosciences) with a mean library size of 400 bp, and 11 million reads were sequenced paired end (2 *50 bp) on a HiSeq. 1500 by the LAFUGA sequencing facility of the Ludwig-Maximilians University Gene Center in Munich. Analyses were performed on the LAFUGA Galaxy web server. Briefly all reads were BLASTed against the sequence of the repair construct with a cutoff of 0.0001. 390 mate reads both BLASTed on the repair construct, and BLAST results were used to infer the length of each insert (Fig. S1F). In 27 cases, only one read of the pair BLASTed on the repair construct. The 27 mate reads were retrieved and BLASTed against the *Drosophila melanogaster* genome (release r6.17) downloaded from Flybase (Gramates et al., 2017) (Fig. S1G).

4.5. Immunochemistry

4.5.1. Antibody production

A polyclonal anti-Yellow antibody was produced at the Ludwig-Maximilians University Veterinary school by immunizing 2 rabbits with a purified Yellow-GST protein produced from the expression vector Dmel-Yellow-GST in pGEX-5 × 1 (a gift from Trisha Wittkopp; (Wittkopp et al., 2002a)). Sera were collected 2 months after immunization and affinity purified.

4.5.2. Western blot

Pupal wings were ground in 2x Laemmli buffer (0.125 M Tris-Cl, pH6.8, 4.1% SDS, 3.1% DTT, 20% glycerol, bromophenol blue), and boiled at 95 °C for 5 min. Protein samples were then spun down and the supernatants were run on a 10% acrylamide SDS-PAGE gel (~6 wings were used per lane). Western blots were performed as in (Wittkopp et al., 2002a), using the rabbit anti-Yellow antibody described above (1:200), a rabbit anti-mCherry antibody (Novus NBP2–25157) (1:2000) and a rabbit H2Av antibody (1:2000) (a gift from Carla Margulies, produced as in (Leach et al., 2000)). The secondary antibody, a goat anti-rabbit IgG-HRP conjugate (Bio-Rad 170–6515) was used at 1:10000. Detection was performed using the Immobilon Western Chemiluminescent HRP substrate (Merck).

4.6. Pigmentation quantification

4.6.1. D. melanogaster wings

Male flies raised at 20 °C were collected upon hatching and left to maturate 5 days at 20 °C for pigmentation analysis of the $y^{mCherry}$, w^{*} line, compared to w^{*} and y^{1} w^{*} flies. For the experiments with *UAS-mgl-shRNA* line, flies were collected after hatching and left to maturate 7 days at 20 °C, then stored in 80% ethanol at − 20 °C until dissection. A single wing per individual was dissected and mounted in Hoyer's medium (Ashburner, 1989). Wings were imaged under a Leica Macroscope equipped with a Manta G-609B/C camera (GigE camera with Sony ICX694, Allied Vision, Exton, PA) driven by nVision software (Impuls Imaging GmbH, Türkheim) using a diffuse back lighting table (DBL-2020-WT, MBJ Imaging, Hamburg) for illumination. The resulting color images were converted to HSB coordinates (Joblove and Greenberg, 1978). Brightness and hue were averaged from a 50-pixel square in the distal part of the wing between veins L2 and L3, using Fiji (Schindelin et al., 2012)).

4.6.2. D. biarmipes wings

Wings of 11 y^{-} and 16 wild-type 5 day-old adult males were prepared, imaged and registered on a reference wing as in (Arnoult et al., 2013). Average intensity profiles represent the average pigmentation intensity (= 255 - gray level) in the compartments between L1 and L2 veins and between L2 and L3 veins (boxed region in Fig. 6A,B) relative to the distance to an arbitrary proximal limit between more pigmented area and wing background. For each individual, the limit was the proximal border of the area defined by a constant threshold above the background average intensity (see examples on Fig. S5). The threshold was defined as the half of the difference between the average intensity inside and outside the spot, averaged across all y^{-} mutant wings. The threshold allows to center the profiles on a given intensity reference. For each point inside the two compartments, the distance to the proximal spot boundary was calculated using the distance transform (Borgefors, 1986). The averaging of pigmentation intensity for each distance bin resulted in a profile of average pigment intensity, the distance coordinate being relative to a comparable reference. This approach is robust to variation in pattern boundary. It allows to

compute an average profile for each individual that integrates the information all along the spot, not just on a single line. The minimum value near the spot boundary of each profile, i. e., the average intensity of the background has been normalized to 0, to allow the comparison of the slope of the increase in pigmentation intensity. Although it does not reflect the perceived spot border for the wild type (Fig. S5A_3), this constant threshold allows to compare, on common reference, the slope of the transition from the background to the pigmented area, by aligning the profiles (Fig. S5A_2–B_2, A_4–B_4).

4.6.3. Wholemount flies

Specimens from Fig. 1I are 5-day old males raised at 20 °C, anaesthetized and imaged as in (Chyb and Gompel, 2013).

4.7. Fluorescent sample preparation and imaging

4.7.1. Wholemount pupae

$y^{mCherry}$; sqh-utrophin::GFP pupae were dissected out of their pupal case, mounted live in Voltalef oil to permit gas exchanges, and imaged in tiles with a Leica TCS SP5 II confocal microscope with the 10 × objective. Tiled image stacks were stitched in Fiji using the Stitching plugin (Preibisch et al., 2009).

4.7.2. Pupal abdomen

65 h, 70 h and 75 h APF *$y^{mCherry}$; sqh-utrophin::GFP* male pupae were dissected from their pupal case, mounted live in Voltalef oil to permit gas exchanges, and imaged with a Leica TCS SP5 II confocal microscope with the 20 × objective, focusing on the A3 and A4 abdominal segments. Image stacks were projected (maximum intensity) and analyzed using Fiji. For each sample, two 150-pixels wide areas, one on each side of the midline, encompassing the whole antero-posterior length of the segment A3 or A4, were blurred using Gaussian blur (sigma 4) and analyzed using the Plot Profile tool of Fiji. The average of all profiles is shown (Fig. S2B-C). The blurred areas of age-matched samples were also projected (average intensity) to get an average of the expression pattern for each segment and at each stage.

4.7.3. Central nervous system

Brains from unsexed L1 (3 *$y^{mCherry}$*, 3 *y^+* controls), L2 (5 *$y^{mCherry}$*, 1 *y^+* control) and L3 (6 *$y^{mCherry}$*, 5 *y^+* controls) larvae as well as 5-day old adult female flies (7 *$y^{mCherry}$*, 5 *$y^{mCherry}$*, *pdf > GFP*; 2 *y^+* controls) were dissected in cold PBS and collected in 1% paraformaldehyde on ice. Following fixation with 4% paraformaldehyde at room temperature (20 min for L1, 30 min for L2 and L3, 45 min for adult brains), brains were washed 3 × 10 min in PBS, 0.1% Triton X-100 and then incubated in blocking solution for 1 h (3% normal goat serum, 0.1% Triton X-100 in PBS). Primary antibodies were incubated overnight at 4 °C in blocking solution. After washing 3 × 20 min in PBS, 0.1% Triton X-100, brains were incubated with secondary antibodies for 4 h at room temperature in blocking solution and again washed in PBS, 0.1% Triton X-100 for 3 × 20 min and 1 × 1 h. All tissues were mounted with Vectashield mounting medium. All microscopic observations were made at a Leica SP8 confocal microscope. Image stacks were analyzed and projected (maximum intensity) using Fiji (Schindelin et al., 2012).

The primary antibodies used were rat anti-N-cadherin (anti-N-cad DN-Ex #8, Developmental Studies Hybridoma Bank, 1:200), Living Colors® rabbit anti-DsRed (Clontech, 1:200) and 75–132 anti-GFP primary antibody (specific to full GFP, monoclonal, NeuroMab, clone N86/38, 1:200). The following secondary antibodies were used: goat anti-rat Alexa 488 (invitrogen, 1:200), goat anti-rabbit Cy3 (Jackson ImmunoResearch, 1:200) and anti-mouse Alexa488 (molecular probes, 1:250), respectively.

4.7.4. Time-lapse of pupae

Male white prepupae (*$y^{mCherry}$, w**) were selected and left to develop at 25 C° for 44 h, then placed individually, ventral side up, in a humid chamber. The chamber was a 55 mm Petri dish coated with humid tissue, covered with parafilm, and with a hatch at the center of the parafilm lid, for imaging with the 10x objective of a Zeiss Imager M2 wide field microscope. The whole pupa was scanned every 450 s under bright field and fluorescent light with a pco sensicam camera driven with a custom camera software (Lim et al., 2016). Imaging was performed for approximately 48 h at 20 °C. Development at 20 °C was assumed to be 1.5 times slower than at 25 °C (Ludwig and Cable, 1933; Powsner, 1935), and developmental times indicated on the figures are equivalent to development at 25 °C. Time-lapse stacks were analyzed using Fiji. For each wing, 6 squares of 12*12 pixels were quantified on the best focused section of the stack and the means of these measures were plotted against time.

4.7.5. Pupal wings

Male white prepupae of 4 genotypes (1. *$y^{mCherry}$, w*;UAS-mCD8::GFP/+; NP3537/+* called "*$y^{mCherry}$, mCD8::GFP*" – 2. *y^+, w*; UAS-ChtVis-Tomato/ UAS-mCD8::GFP; NP3537/+* called "*ChtVis-Tomato, mCD8::GFP*" – 3. *y^+, w*;UAS-mCD8::GFP/+; NP3537/+* called "*y^+ mCD8::GFP*" – 4. *$y^{mCherry}$, w*;UAS-mCD8::GFP/UAS- mgl-shRNA; NP3537/+* called "*$y^{mCherry}$, mgl RNAi*") were selected and aged at 25 °C until the appropriate developmental point. They were then dissected out of the pupal case, wings were removed from their envelope and allowed to unfold in distilled water. They were then fixed in PBS 4% PFA for 30 min at room temperature, washed in PBS and mounted in Vectashield with DAPI (Vector Laboratories). They were then imaged with a Leica TCS SP5 II confocal microscope, using the 63 × objective. Stacks were resliced along the z-axis in Fiji, accounting for the chromatic shift. The imaging of *y^+, mCD8::GFP* wings revealed low levels of autofluorescence, much weaker than the signal produced by Yellow::mCherry (Fig. S3).

All images were processed with Adobe Photoshop, using linear enhancement as well as gamma correction.

Acknowledgements

We thank Haris Khan and Carla Margulies for help with Western blots and for sharing reagents, Nadin Memar for help with time-lapse imaging, Karin Merk and Klaus Förstemann for test of the sgRNAs in cell culture, Helmut Blum and Stefan Krebs of the Gene Center Genomics Unit (LMU, Munich) for library preparation and Illumina sequencing, Yan Jaszczyszyn and Cloelia Dard-Dascot of the I2BC High Throughput Sequencing Core Facility for help with the analysis of the sequencing data. We thank Frank Schnorrer, Paul Adler Anne Classen, Jean-Paul Vincent, Aaron Voigt and Barry Thompson for sharing fly stocks and reagents. We are grateful to Patricia Wittkopp and Artyom Kopp for constructive comments on the manuscript. We also thank Irina Hein for discussion in the early phase of the project and Sabine Radetzki for technical support with the molecular biology. Stocks obtained from the Bloomington Drosophila Stock Center (NIH P40OD018537) were used in this study.

Funding

This project has received funding from the European Union's Horizon 2020 research and innovation programme under the Marie Sklodowska-Curie grant agreement No 701691, and from the Ludwig-Maximilians University of Munich. LR was supported by the Amgen Scholar program of the LMU; JK is supported by the Max Planck Society; YX is supported by a China Scholarship Council Ph.D. fellowship.

Appendix A. Supporting information

Supplementary data associated with this article can be found in the online version at doi:10.1016/j.ydbio.2018.04.003.

References

Arnoult, L., Su, K.F., Manoel, D., Minervino, C., Magrina, J., Gompel, N., Prud'homme, B., 2013. Emergence and diversification of fly pigmentation through evolution of a gene regulatory module. Science 339, 1423–1426.

Ashburner, M., 1989. Drosophila: A Laboratory Handbook and Manual. Two volumes.

Baena-Lopez, L.A., Alexandre, C., Mitchell, A., Pasakarnis, L., Vincent, J.P., 2013. Accelerated homologous recombination and subsequent genome modification in Drosophila. Development 140, 4818–4825.

Bassett, A., Liu, J.L., 2014. CRISPR/Cas9 mediated genome engineering in Drosophila. Methods 69, 128–136.

Bassett, A.R., Tibbit, C., Ponting, C.P., Liu, J.L., 2013. Highly efficient targeted mutagenesis of Drosophila with the CRISPR/Cas9 system. Cell Rep. 4, 220–228.

Bastock, M., 1956. A gene mutation which changes behavior pattern. Evolution 10, 421–439.

Borgefors, G., 1986. Distance transformations in digital images. Comput. Vision., Graph., Image Process. 34, 344–371.

Brehme, K.S., 1941. The effect of adult body color mutations upon the Larva of *Drosophila melanogaster*. Proc. Natl. Acad. Sci. USA 27, 254–261.

Bridges, C.B., Morgan, T.H., 1919. Contributions to the genetics of *Drosophila melanogaster*. Carne. Inst. Wash. Publ. 278, 123–304.

Bridges, C.B., Morgan, T.H., 1923. The third-chromosome group of mutant characters of *Drosophila melanogaster*. Carne. Inst. Wash. Publ. 327, 1–251.

Budnik, V., White, K., 1987. Genetic dissection of dopamine and serotonin synthesis in the nervous system of Drosophila melanogaster. J. Neurogenet. 4, 309–314.

Chyb, S., Gompel, N., 2013. Atlas of Drosophila morphology: Wild-type and Classical Mutants. Academic Press, London; Waltham, MA.

Czapla, T.H., Hopkins, T.L., Kramer, K.J., 1990. Catecholamines and related o-diphenols in cockroach hemolymph and cuticle during sclerotization and melanization: comparative studies on the order Dictyoptera. J. Comp. Physiol. B, Biochem. Syst. Environ. Physiol. 160, 175–181.

Drapeau, M.D., 2003. A novel hypothesis on the biochemical role of the Drosophila Yellow protein. Biochem. Biophys. Res. Commun. 311, 1–3.

Drapeau, M.D., Cyran, S.A., Viering, M.M., Geyer, P.K., Long, A.D., 2006. A cis-regulatory sequence within the yellow locus of *Drosophila melanogaster* required for normal male mating success. Genetics 172, 1009–1030.

Drapeau, M.D., Radovic, A., Wittkopp, P.J., Long, A.D., 2003. A gene necessary for normal male courtship, yellow, acts downstream of fruitless in the *Drosophila melanogaster* larval brain. J. Neurobiol. 55, 53–72.

Edwards, K.A., Doescher, L.T., Kaneshiro, K.Y., Yamamoto, D., 2007. A database of wing diversity in the Hawaiian Drosophila. PLoS One 2, e487.

Geyer, P.K., Spana, C., Corces, V.G., 1986. On the molecular mechanism of gypsy-induced mutations at the yellow locus of *Drosophila melanogaster*. EMBO J. 5, 2657–2662.

Gibert, J.M., Mouchel-Vielh, E., Peronnet, F., 2017. Modulation of yellow expression contributes to thermal plasticity of female abdominal pigmentation in Drosophila melanogaster. Sci. Rep. 7, 43370.

Gompel, N., Carroll, S.B., 2003. Genetic mechanisms and constraints governing the evolution of correlated traits in drosophilid flies. Nature 424, 931–935.

Gompel, N., Prud'homme, B., Wittkopp, P.J., Kassner, V.A., Carroll, S.B., 2005. Chance caught on the wing: cis-regulatory evolution and the origin of pigment patterns in Drosophila. Nature 433, 481–487.

Gramates, L.S., Marygold, S.J., Santos, G.D., Urbano, J.M., Antonazzo, G., Matthews, B.B., Rey, A.J., Tabone, C.J., Crosby, M.A., Emmert, D.B., Falls, K., Goodman, J.L., Hu, Y., Ponting, L., Schroeder, A.J., Strelets, V.B., Thurmond, J., Zhou, P., the FlyBase, C., 2017. FlyBase at 25: looking to the future. Nucleic Acids Res. 45, D663–D671.

Hannah, A.M., 1953. Non-autonomy of yellow in gynandromorphs of Drosophila melanogaster. J. Exp. Zool. 123, 523–560.

Helfrich-Forster, C., Homberg, U., 1993. Pigment-dispersing hormone-immunoreactive neurons in the nervous system of wild-type *Drosophila melanogaster* and of several mutants with altered circadian rhythmicity. J. Comp. Neurol. 337, 177–190.

Housden, B.E., Valvezan, A.J., Kelley, C., Sopko, R., Hu, Y., Roesel, C., Lin, S., Buckner, M., Tao, R., Yilmazel, B., Mohr, S.E., Manning, B.D., Perrimon, N., 2015. Identification of potential drug targets for tuberous sclerosis complex by synthetic screens combining CRISPR-based knockouts with RNAi. Sci. Signal. 8, rs9.

Jeong, S., Rokas, A., Carroll, S.B., 2006. Regulation of body pigmentation by the Abdominal-B Hox protein and its gain and loss in Drosophila evolution. Cell 125, 1387–1399.

Joblove, G., Greenberg, D.P., 1978. Color spaces for computer graphics. Comput. Graph. 12, 20–25.

Jurgens, G., Wieschaus, E., Nusslein-Volhard, C., Kluding, H., 1984. Mutations affecting the pattern of the larval cuticle in *Drosophila melanogaster*: II. Zygotic loci on the third chromosome. Wilhelm. Roux's. Arch. Dev. Biol. 193, 283–295.

Kiger, J.A., Jr., Natzle, J.E., Kimbrell, D.A., Paddy, M.R., Kleinhesselink, K., Green, M.M., 2007. Tissue remodeling during maturation of the Drosophila wing. Dev. Biol. 301, 178–191.

Kornezos, A., Chia, W., 1992. Apical secretion and association of the Drosophila yellow gene product with developing larval cuticle structures during embryogenesis. Mol. General. Genet.: MGG 235, 397–405.

Kronforst, M.R., Barsh, G.S., Kopp, A., Mallet, J., Monteiro, A., Mullen, S.P., Protas, M., Rosenblum, E.B., Schneider, C.J., Hoekstra, H.E., 2012. Unraveling the thread of nature's tapestry: the genetics of diversity and convergence in animal pigmentation. Pigment Cell Melanoma Res. 25, 411–433.

Kronforst, M.R., Papa, R., 2015. The functional basis of wing patterning in Heliconius butterflies: the molecules behind mimicry. Genetics 200, 1–19.

Leach, T.J., Mazzeo, M., Chotkowski, H.L., Madigan, J.P., Wotring, M.G., Glaser, R.L., 2000. Histone H2A.Z is widely but nonrandomly distributed in chromosomes of *Drosophila melanogaster*. J. Biol. Chem. 275, 23267–23272.

Lee, T., Luo, L., 1999. Mosaic analysis with a repressible cell marker for studies of gene function in neuronal morphogenesis. Neuron 22, 451–461.

Li, J., Christensen, B.M., 2011. Biological function of insect yellow gene family. In: Liu, T., Kang, L. (Eds.), Recent Advances in Entomological Research.. Springer, Berlin, Heidelberg.

Lim, M.A., Chitturi, J., Laskova, V., Meng, J., Findeis, D., Wiekenberg, A., Mulcahy, B., Luo, L., Li, Y., Lu, Y., Hung, W., Qu, Y., Ho, C.Y., Holmyard, D., Ji, N., McWhirter, R., Samuel, A.D., Miller, D.M., Schnabel, R., Calarco, J.A., Zhen, M., 2016. Neuroendocrine modulation sustains the C. elegans forward motor state. eLife 5.

Lindsley, D.L., Grell, E.H., 1968. Genetic variations of Drosophila melanogaster.

Locke, M., 2001. The Wigglesworth lecture: insects for studying fundamental problems in biology. J. Insect Physiol. 47, 495–507.

Ludwig, D., Cable, R.M., 1933. The effect of alternating temperatures on the pupal development of *Drosophila melanogaster* Meigen. Physiol. Zool. 6, 493–508.

Mason, H.S., 1955. Comparative biochemistry of the phenolase complex. Adv. Enzymol. Relat. Subj. Biochem. 16, 105–184.

Massey, J.H., Wittkopp, P.J., 2016. The genetic basis of pigmentation differences within and between Drosophila species. Curr. Top. Dev. Biol. 119, 27–61.

Morgan, T.H., Bridges, C.B., 1916. Sex-linked Inheritance in Drosophila 237. Carnegie Institute of Washington Publication, 1–88.

Moussian, B., 2010. Recent advances in understanding mechanisms of insect cuticle differentiation. Insect Biochem. Mol. Biol. 40, 363–375.

Nash, W.G., 1976. Patterns of pigmentation color states regulated by the y locus in *Drosophila melanogaster*. Dev. Biol. 48, 336–343.

Park, J.H., Helfrich-Forster, C., Lee, G., Liu, L., Rosbash, M., Hall, J.C., 2000. Differential regulation of circadian pacemaker output by separate clock genes in Drosophila. Proc. Natl. Acad. Sci. USA 97, 3608–3613.

Pavlopoulos, A., Akam, M., 2011. Hox gene Ultrabithorax regulates distinct sets of target genes at successive stages of Drosophila haltere morphogenesis. Proc. Natl. Acad. Sci. USA 108, 2855–2860.

Port, F., Chen, H.M., Lee, T., Bullock, S.L., 2014. Optimized CRISPR/Cas tools for efficient germline and somatic genome engineering in Drosophila. Proc. Natl. Acad. Sci. USA 111, E2967–E2976.

Powsner, L., 1935. The effects of temperature on the durations of the developmental stages of *Drosophila melanogaster*. Physiol. Zool. 8, 474–520.

Preibisch, S., Saalfeld, S., Tomancak, P., 2009. Globally optimal stitching of tiled 3D microscopic image acquisitions. Bioinformatics 25, 1463–1465.

Prud'homme, B., Gompel, N., Rokas, A., Kassner, V.A., Williams, T.M., Yeh, S.D., True, J.R., Carroll, S.B., 2006. Repeated morphological evolution through cis-regulatory changes in a pleiotropic gene. Nature 440, 1050–1053.

Radovic, A., Wittkopp, P.J., Long, A.D., Drapeau, M.D., 2002. Immunohistochemical colocalization of Yellow and male-specific Fruitless in *Drosophila melanogaster* neuroblasts. Biochem. Biophys. Res. Commun. 293, 1262–1264.

Rauzi, M., Lenne, P.F., Lecuit, T., 2010. Planar polarized actomyosin contractile flows control epithelial junction remodelling. Nature 468, 1110–1114.

Rebeiz, M., Pool, J.E., Kassner, V.A., Aquadro, C.F., Carroll, S.B., 2009. Stepwise modification of a modular enhancer underlies adaptation in a Drosophila population. Science 326, 1663–1667.

Riedel, F., Vorkel, D., Eaton, S., 2011. Megalin-dependent yellow endocytosis restricts melanization in the Drosophila cuticle. Development 138, 149–158.

Schindelin, J., Arganda-Carreras, I., Frise, E., Kaynig, V., Longair, M., Pietzsch, T., Preibisch, S., Rueden, C., Saalfeld, S., Schmid, B., Tinevez, J.Y., White, D.J., Hartenstein, V., Eliceiri, K., Tomancak, P., Cardona, A., 2012. Fiji: an open-source platform for biological-image analysis. Nat. Methods 9, 676–682.

Shaner, N.C., Campbell, R.E., Steinbach, P.A., Giepmans, B.N., Palmer, A.E., Tsien, R.Y., 2004. Improved monomeric red, orange and yellow fluorescent proteins derived from Discosoma sp. red fluorescent protein. Nat. Biotechnol. 22, 1567–1572.

Sherald, A.F., 1980. Sclerotization and coloration of the insect cuticle. Experientia 36, 143–146.

Sobala, L.F., Adler, P.N., 2016. The gene expression program for the formation of wing cuticle in Drosophila. PLoS Genet. 12, e1006100.

Sobala, L.F., Wang, Y., Adler, P.N., 2015. ChtVis-Tomato, a genetic reporter for in vivo visualization of chitin deposition in Drosophila. Development 142, 3974–3981.

Sobala, L.F., Wang, Y., Adler, P.N., 2016. Correction: ChtVis-Tomato, a genetic reporter for in vivo visualization of chitin deposition in Drosophila. Development 143, 3638.

Stockinger, P., Kvitsiani, D., Rotkopf, S., Tirian, L., Dickson, B.J., 2005. Neural circuitry that governs Drosophila male courtship behavior. Cell 121, 795–807.

Sugumaran, M., Barek, H., 2016. Critical analysis of the melanogenic pathway in insects and higher animals. Int. J. Mol. Sci. 17.

True, J.R., Edwards, K.A., Yamamoto, D., Carroll, S.B., 1999. Drosophila wing melanin patterns form by vein-dependent elaboration of enzymatic prepatterns. Curr. Biol.: CB 9, 1382–1391.

Waldo, G.S., Standish, B.M., Berendzen, J., Terwilliger, T.C., 1999. Rapid protein-folding assay using green fluorescent protein. Nat. Biotechnol. 17, 691–695.

Walter, M.F., Black, B.C., Afshar, G., Kermabon, A.Y., Wright, T.R., Biessmann, H., 1991. Temporal and spatial expression of the yellow gene in correlation with cuticle formation and dopa decarboxylase activity in Drosophila development. Dev. Biol. 147, 32–45.

Werner, T., Koshikawa, S., Williams, T.M., Carroll, S.B., 2010. Generation of a novel wing colour pattern by the Wingless morphogen. Nature 464, 1143–1148.

Williams, T.M., Selegue, J.E., Werner, T., Gompel, N., Kopp, A., Carroll, S.B., 2008. The regulation and evolution of a genetic switch controlling sexually dimorphic traits in

Drosophila. Cell 134, 610–623.
Wilson, J.S., Jahner, J.P., Forister, M.L., Sheehan, E.S., Williams, K.A., Pitts, J.P., 2015. North American velvet ants form one of the world's largest known Mullerian mimicry complexes. Curr. Biol.: CB 25, R704–R706.
Wittkopp, P.J., Carroll, S.B., Kopp, A., 2003. Evolution in black and white: genetic control of pigment patterns in Drosophila. Trends Genet.: TIG 19, 495–504.
Wittkopp, P.J., True, J.R., Carroll, S.B., 2002a. Reciprocal functions of the Drosophila yellow and ebony proteins in the development and evolution of pigment patterns. Development 129, 1849–1858.
Wittkopp, P.J., Vaccaro, K., Carroll, S.B., 2002b. Evolution of yellow gene regulation and pigmentation in Drosophila. Curr. Biol.: CB 12, 1547–1556.
Wright, T.R., 1987. The genetics of biogenic amine metabolism, sclerotization, and melanization in *Drosophila melanogaster*. Adv. Genet. 24, 127–222.